

MRSI Brain Temperature Mapping Using Machine Learning

Dhritiman Das^{1,2,3,4}, Michael J Thrippleton³, Mike E Davies², Rolf F Schulte⁴,
Bjoern H Menze¹, Ian Marshall³

¹Department of Computer Science, Technical University of Munich, Germany

²Institute for Digital Communications, University of Edinburgh

³Centre for Clinical Brain Sciences, University of Edinburgh

⁴GE Global Research Europe, Munich, Germany

Abstract. We propose a machine-learning framework for brain temperature estimation in MRSI using human in-vivo data from 1.5T and 3T scanners. We consider the chemical-shift based method as our benchmark and compare our results against it. Our framework, based on random-forest regression, performs a K-fold cross validation on the MRSI dataset which includes (1) learning the spectral features (including the chemical-shift) from the subjects; (2) obtaining brain temperature estimates and computing the error over the corresponding jMRUI-fitted chemical-shift based estimates. Compared to jMRUI, our method, after training, gives a low estimation error and a 30-fold improvement in estimation speed per patient.

1 Purpose

Temperature is an important physiological parameter used in the care and treatment of brain-injured patients. Non-invasive mapping of the brain temperature using MRSI can help in assessing the effects of conditions such as acute ischaemic stroke and blood circulation disorders. Prior work has focused on measurement of brain temperature using the chemical-shift method [10] (among other indicators such as proton density [6], relaxation times [8], diffusion coefficient [2]). As an alternative, we propose a simple yet effective machine-learning approach using random-forest regression for brain temperature mapping which is evaluated on human in-vivo data acquired from both 1.5T and 3T scanners. Our training model accounts for the trends in spectral pattern, in addition to the chemical-shift, to predict the brain temperature. This is the first application-to the best of our knowledge- of machine learning towards brain temperature mapping in MRSI.

2 Methods

Random Forests [4] have been used in MRSI towards classification [1][7] and quantification [5] of spectral data. These involve multiple forests comprising of a

set of binary trees. For training, splits are created in each tree based on random subsets of the feature variables and piecewise linear regression is performed over the input data. The process involves seeking best prediction at every node and using thresholding to further propagate data points till they reach the end of the tree. Subsequently the weighted average of the prediction from each tree is taken to give a single output estimate.

Subjects 10 healthy, male volunteers in the age range of 23-40 years (mean +/- SD, 30.5 +/- 5.2 years) were invited for scanning on 3 occasions and underwent 4 MRSI scans each on both **1.5T** (PRESS sequence, **TR/TE** = 1000/144ms, **FOV** = 300mm², 24-step phase encoding in both in-plane directions) and **3T** (semi-LASER PRESS sequence, **TR/TE** = 1700/144ms, **FOV** = 256mm²) scanners during each visit. Data was zero-filled (in k-space), interpolated to 32x32 voxels and corrected for eddy and phase correction. Additional details can be found in [10]. The data was fitted using the AMARES algorithm ([9]) and voxels with poor quality of NAA-fits and/or water resonance distortions were rejected. Total spectra per fold included approximately 1800 training and 150 test-spectra/subject respectively.

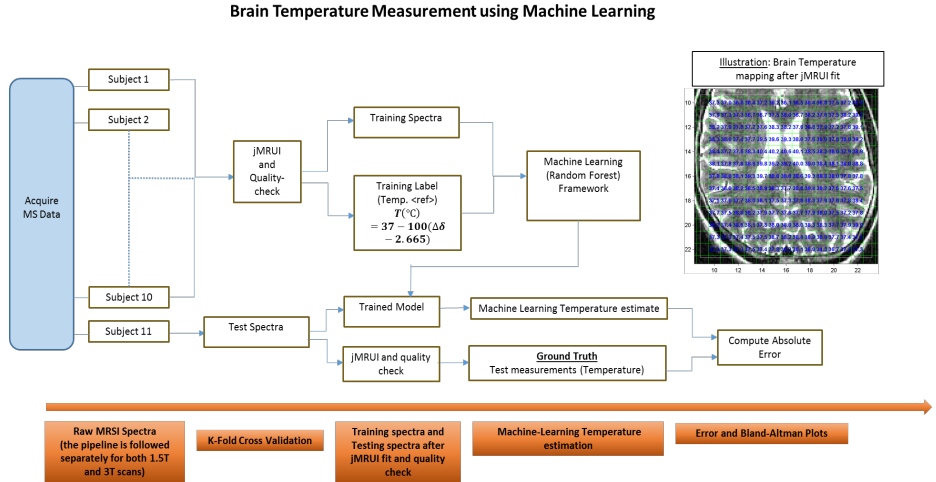


Fig. 1. Pipeline for Machine Learning based brain temperature measurement. Using the K-fold cross validation approach, this method is repeated using spectra from each of the 10 subject as test spectra. The temperature measured using the jMRUI-based chemical-shift method is considered to be the ground-truth. An illustrated image also shows the brain temperature estimation for a MRS image acquired from a sample patient (after fitting and pre-quality check.)

In MRSI, The time-domain complex signal of a nucleus is given by:

$$S(t) = \int p(\omega)\exp(-i\Phi)\exp(-t/T_2^*)d\omega. \quad (1)$$

, and the corresponding frequency-domain spectrum is given by $S(\omega)$.

As shown in Fig. 1, we aim to perform the inverse signal modeling where we have a training dataset $D = (S_i(\omega), T_i)$, $i \in [1, N]$, where N is the total number of training spectra from 10 subjects. $S_i(\omega)$ represents the training spectral data while T_i represents the corresponding voxel-wise chemical-shift brain temperature estimates obtained after-fitting (in °C) [10]. For the purpose of ensuring homogeneity, we train spectra that have passed the quality control measure post-fitting (as mentioned earlier).

The training labels correspond to the temperature evaluated using the formula mentioned in [10] wherein the chemical shift is calculated after fitting the spectra using jMRUI [9]. Using the dataset from each scanner, we perform a separate K-fold cross validation evaluation comprising 10 folds (number of trees = 100 and mTry = 128) wherein each fold we generate a training set from randomly selected 9 subjects and test on spectra, $S_j(\omega)$, from the remaining subject to obtain the brain temperature estimates \hat{T}_j . The corresponding chemical-shift based temperature estimates T_j serve as the ground-truth, $j \in [1, M]$ where M is the total number of test spectra.

Error Calculation. For our experiments, given the estimate \hat{T}_j and the test temperature T_j for a given subject, the estimate error \hat{E}_j (in °C) can be calculated as,

$$\hat{E}_j = ||\hat{T}_j - T_j|| \quad (2)$$

This approach helps us to assess the absolute change in brain temperature estimates over the ground-truth values. The corresponding box plots and Bland-Altman plots [3] for a sample subject are also shown to indicate the difference in temperature patterns.

3 Results

The temperature-mapping estimates for a sample subject using both the chemical-shift and the random-forest methods has been shown in **Fig. 2**. The mean relative error plots for each subject is shown in **Fig. 3**. Using the Bland-Altman method, we observe a strong correlation between the chemical-shift estimates (using jMRUI) and the random-forest estimates for a sample patient (**Fig. 4**). **Speed:** Training time per fold is 1 minute. While the jMRUI fitting takes 5 minutes per subject, our proposed framework, after training, takes only 10 seconds leading to a **30x** improvement in speed.

4 Discussion

In **Fig. 2**, the temperature difference between the 2 methods are minimal leading to a low-error. A slightly higher error can be seen around the CSF regions and at the edges which are most likely due to the variations in spectral pattern in these areas. Such spectra are fewer in number (post quality-check) and therefore the framework is insufficiently trained to identify similar spectral patterns. The

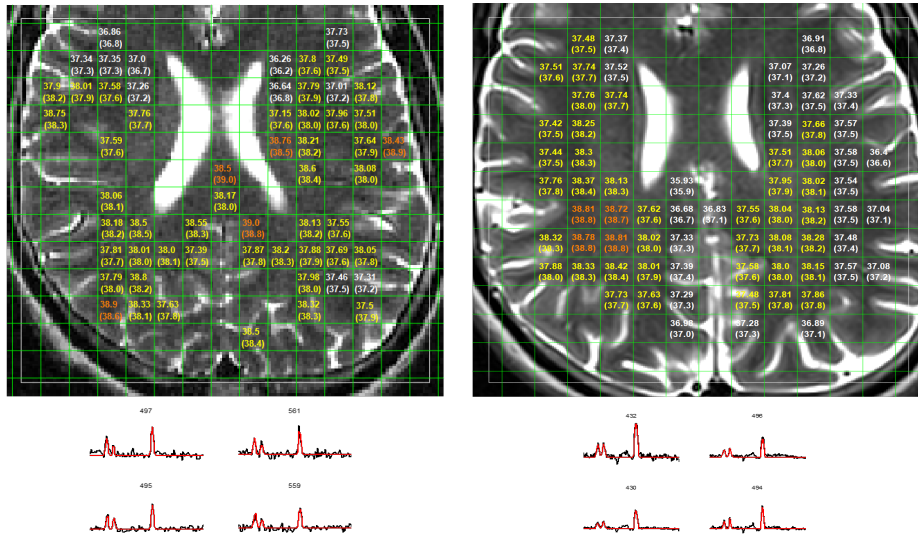


Fig. 2. T2-weighted images overlaid with MRSI excitation volumes and brain temperature estimates (in $^{\circ}\text{C}$) for a sample subject using MRSI data from both 1.5T (**Left**) and 3T (**Right**) scanners [10]. The values in brackets represent the estimates using the chemical-shift method while the other values represent the random-forest based temperature estimates (machine-learning). The spectra shown below each image represent the acquired (**Red**) and simulated (**Black**) corresponding to a set of sample voxels.

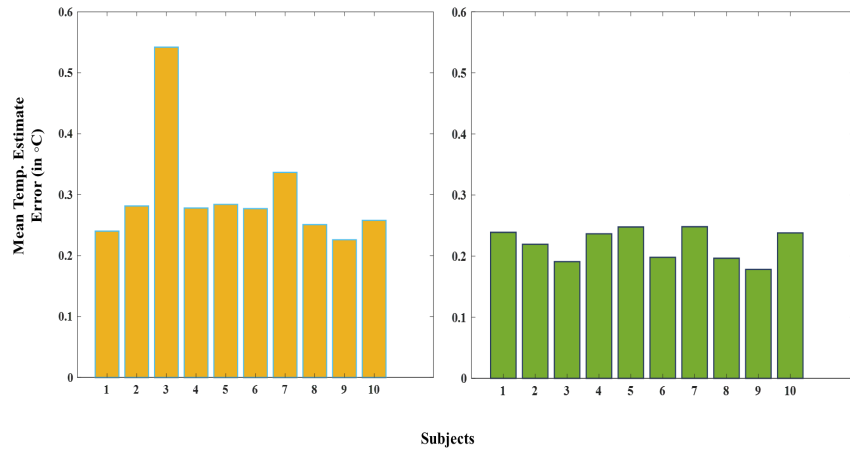


Fig. 3. Mean temperature estimate errors (in $^{\circ}\text{C}$) for each of the 10 subjects from the (**Left**) 1.5T and (**Right**) 3T scanners. In the 1.5T scanner, one of the subjects exhibited a higher error compared to the others. Comparing the 2 plots, the 3T spectra being higher in quality and spatial resolution gives a lower error than the 1.5T data. The difference, though, is not substantial.

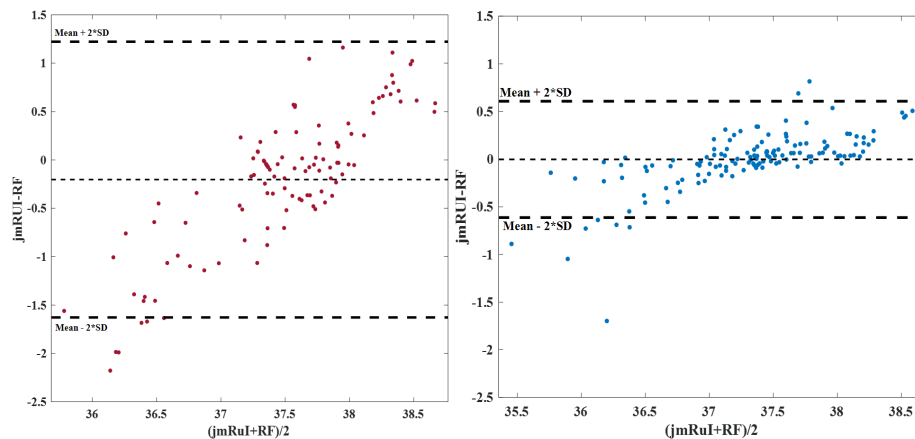


Fig. 4. Bland-Altman correlation plots [3] for a sample subjects using data from **(Left)** 1.5T and **(Right)** 3T scanners. The X-Axis represents the average of the chemical-shift (using jMRUI) and random-forest (RF) estimates while the Y-axis represents their difference. The 3T data exhibits a better correlation than the 1.5T data.

outliers observed in the corresponding Bland-Altman plots shown in **Fig. 4** also correspond to these regions. The mean-error plots, shown in **Fig. 3**, correspond to an overall mean error of **0.29 °C** for the 1.5T data and **0.202 °C** for the 3T data (due to better spectral quality and resolution). Estimates for Subject 3 exhibited a slightly higher error for the 1.5T data but this issue wasn't present while evaluating the corresponding 3T data.

Future work would involve performing extensive phantom studies for a better assessment between the machine-learning and chemical shift methods. More robust frameworks involving deep-learning based methods can be used to improve the accuracy of temperature estimation.

Acknowledgements. The research leading to these results has received funding from the European Union's H2020 Framework Programme (H2020-MSCA-ITN-2014) under grant agreement n 642685 MacSeNet.

References

1. Pedrosa de Barros, N., McKinley, R., Wiest, R., Slotboom, J.: Improving labeling efficiency in automatic quality control of mrsi data. *Magnetic Resonance in Medicine* pp. n/a–n/a (2017), <http://dx.doi.org/10.1002/mrm.26618>
2. Bihan, D.L., Delannoy, J., Levin, R.L.: Temperature mapping with mr imaging of molecular diffusion: application to hyperthermia. *Radiology* 171(3), 853–857 (1989), <https://doi.org/10.1148/radiology.171.3.2717764>, PMID: 2717764
3. Bland, J.M., Altman, D.: Statistical methods for assessing agreement between two methods of clinical measurement. *The Lancet* 327(8476), 307 – 310 (1986), <http://www.sciencedirect.com/science/article/pii/S0140673686908378>, originally published as Volume 1, Issue 8476

4. Breiman, L.: Random forests. *Machine Learning* 45(1), 5–32 (2001), <http://dx.doi.org/10.1023/A:1010933404324>
5. Das, D., Coello, E., Schulte, R.F., Menze, B.H.: Quantification of Metabolites in Magnetic Resonance Spectroscopic Imaging Using Machine Learning, pp. 462–470. Springer International Publishing, Cham (2017), https://doi.org/10.1007/978-3-319-66179-7_53
6. Kuroda, K., Suzuki, Y., Ishihara, Y., Okamoto, K., Suzuki, Y.: Temperature mapping using water proton chemical shift obtained with 3d-mrsi: Feasibility in vivo. *Magnetic Resonance in Medicine* 35(1), 20–29 (1996), <http://dx.doi.org/10.1002/mrm.1910350105>
7. Menze, B.H., Kelm, B.M., Weber, M.A., Bachert, P., Hamprecht, F.A.: Mimicking the human expert: Pattern recognition for an automated assessment of data quality in mr spectroscopic images. *Magnetic Resonance in Medicine* 59(6), 1457–1466 (2008), <http://dx.doi.org/10.1002/mrm.21519>
8. Parker, D.L.: Applications of nmr imaging in hyperthermia: An evaluation of the potential for localized tissue heating and noninvasive temperature monitoring. *IEEE Transactions on Biomedical Engineering* BME-31(1), 161–167 (Jan 1984)
9. Stefan, D., Cesare, F.D., Andrasescu, A., Popa, E., Lazariev, A., Vescovo, E., Strbak, O., Williams, S., Starcuk, Z., Cabanas, M., van Ormondt, D., Graveron-Demilly, D.: Quantitation of magnetic resonance spectroscopy signals: the jmrui software package. *Measurement Science and Technology* 20(10), 104035 (2009), <http://stacks.iop.org/0957-0233/20/i=10/a=104035>
10. Thrippleton, M.J., Parikh, J., Harris, B.A., Hammer, S.J., Semple, S.I.K., Andrews, P.J.D., Wardlaw, J.M., Marshall, I.: Reliability of mrsi brain temperature mapping at 1.5 and 3 t. *NMR in Biomedicine* 27(2), 183–190 (2014), <http://dx.doi.org/10.1002/nbm.3050>, nBM-13-0102.R2